Adams Metal Oxide Catalysts for Solar Driven Water Splitting

ARTICLE

Adams Metal Oxide Catalysts for Solar Driven Water Splitting

M. P. Browne, [a] C. O'Rourke [a] Nathan Wells[a] and A. Mills*[a]

Abstract: The wide spread utilisation of solar driven water is hindered by the use of expensive and unstable materials. Herein, we show that highly active earth abundant metal oxide oxygen and hydrogen evolution electrocatalysts can be synthesised using the Adams method, in which the metal salts are oxidised in a melt of sodium nitrate and that such oxides are usually highly crystalline powders with high specific surface areas. Disc electrodes of the Adams method metal oxides: RuO_2, Mn_2O_3, Co_3O_4 and NiO are prepared using a recently reported mechanical, solvent-free method, involving pressing a mixture of the metal oxide and a small amount (5 wt%) of PTFE powder. Each electrode is tested as an electrode for the hydrogen evolution reaction, HER, and oxygen evolution reaction, OER, in 1 M NaOH. In the former role, Mn_2O_3 appears better than a platinum wire electrode (overpotential at 10 mA cm^{-2}, η_{10}, = 61 mV, cf. 70 mV, for Pt). In the OER study, although RuO_2 is the best electrocatalyst, η_{10}, = 267 mV, Co_3O_4 is also very effective, η_{10}, = 330 mV. Using Mn_2O_3 as the cathode and Co_3O_4 as the anode, a silicon solar cell is used to photocleave water into H_2 and O_2.

Introduction

A vast amount of current research is focused on finding alternative energy sources to combat the World's rapidly depleting fossil fuel reserves[[1] Solar driven electrolytic water splitting is an attractive process for producing clean hydrogen, from which heat or electricity can be easily derived.[2] Unfortunately, the best electrocatalysts for water splitting belong are platinum group metal, i.e. PGM, based, namely: RuO_2 or IrO_2 for water oxidation and Pt for hydrogen evolution, and as a result they are expensive and so present problems of scale up and global utilisation.

Not surprisingly there are extensive efforts to find Earth-abundant alternatives to the PGM's used to mediate the Hydrogen Evolution Reaction (HER)[3] and the Oxygen Evolution Reaction (OER)[4], since the large scale utilisation of water splitting depends on the development of less expensive materials with similar activities to the previously identified PGM-based electrocatalysts.[5]

In the electrochemical characterisation of potential water splitting electrocatalysts, a commonly reported characteristic is overpotential (η), for the HER, or OER, at a current density of -10 mA cm^{-2} or 10 mA cm^{-2},respectively, which is often denoted as η_{-10} or η_{10}, respectively.[2d], since a current density of 10 mA cm^{-2} is that associated with an efficient solar driven electrolysis cell.[6]

[a] Dr. M. P. Browne, Dr. C. O'Rourke, DR. N. Wells and Prof. A. Mills
School of Chemistry and Chemical Engineering,
Queens University Belfast,
UK.

E-mail: andrew.mills@qub.ac.uk

Typical η_{-10} values in the literature for Pt as a HER catalyst are in the region of 0.10 V vs. the Reversible Hydrogen Electrode (RHE),[7] while commercial RuO_2 materials for the OER exhibit η_{10} values of ca. 0.36 V.[8] Therefore, the overall voltage required to drive a solar-driven water splitting cell comprising of a Pt cathode and a RuO_2 anode system, would be ca. 1.69 V vs. RHE.

The *ideal* Earth-abundant electrocatalyst should outperform the more expensive and established PGM electrocatalysts and so should have a large density of active sites with respect to the material's surface area, or more particularly, its active electrochemical surface area (ECSA). The fabrication of high surface area (powdered) materials can be achieved by the Adams method, which involves the oxidation of the metal salt in molten sodium nitrate. This fabrication method has many advantages over other synthetic routes, most commonly the thermal oxidation of metal salts in air, that have been used in the past to produce powdered metal oxides, in that it is fast (0.5 h) and produces highly crystalline materials, often with high surface areas.[9] In contrast, hydrothermal methods usually produce high surface area, highly defective, often amorphous metal oxides, that often require a subsequent annealing step. Intriguingly, despite these attractive features, there are few studies of the use of this method to produce anything other than Adams PGM oxides.[9-10] For example, Oakland et al., has reported that IrO_2, synthesised by the Adams method, is superior in terms of OER performance, than commercial IrO_2/TiO_2.[10b] In this latter study, this improved performance of the IrO_2 Adams powder was attributed to its large BET surface area, 150 m^2 $g^{-1,}$ which, in turn, is attributed to the method of synthesis.[10b]

A great deal of research into new electrocatalysts for water splitting, especially into those for the most challenging four electron oxidation of water, involves the synthesis of the electrocatalytic material often in powder form, and such powders obviously require deposition onto an appropriate conducting support, or preparation in a form that can be used as an electrode. Geiger et al. recently reported that the commonly used electrode support for the deposition of powered electrocatalystswork, i.e. Glassy Carbon (GC) electrodes, are not good substrates for supporting water oxidation electrocatalytic powdered materials, due to the poor electrochemical stability of the underlying GC disc material.[11] This study reported[16] that when polarised for short time periods (0.5 h) the activity of a IrO_2/GC electrode is decreased. However, *in-situ* Inductively Coupled Plasma (ICP) measurements revealed that minimal amounts of the IrO_2 catalyst (1.3% of catalyst deposited) were detected in the solution, indicating that the observed loss in activity ws not due to the physical or chemical loss of the active material. Instead, the authors suggest [16] that the loss in activity is due to the formation of a passivation layer between the underlying GC electrode support and the catalyst. Similarly, Sayeed et al. reported a huge decrease in activity of electrodeposited $FeCoNi_x$ on GC supports for the OER after multi-cycling in 0.1M NaOH, while the same

material on metal supports (Au, Pd and Cu) retained its activity after the same number of cycles.[12]

Another disadvantage with carbon based electrodes, as a support for water oxidation catalysts, is the degradation of the carbon under the high potentials associated with the OER.[[13]] Jaramillo *et al.* previously showed evidence of carbon degradation from a GC electrode during tests of the Faradaic efficiency of a number of different metal oxides for water oxidation.[[2d]] As a result, a significant percentage of the current observed in a linear sweep voltammogram of such powder electrocatalysts, deposited onto a GC electrode, is likely due to the oxidation of the carbon support and not the evolution of oxygen, which obviously is very undesirable. The results from the above studies suggest that GC, at least, is not an ideal supporting substrate for water oxidation catalysts, despite its widespread use.[[2c, 2d]]

Recently, our group published a new mechanical, high surface area and solvent-free electrode fabrication method, involving pressed discs of powdered electrocatalysts, bound by a small amount of polymer (PTFE) support; this method provides an alternative to the more commonly employed drop-casting onto GC disc method for making OER electrodes from powdered electrocatalysts.[[14]] Unlike other methods, the pressed disc method allows the OER features of any powdered material to be probed readily without suffering interferences from solvents and conductive supports such as carbon nanotubes and Nafion. As a support, it uses a thin pressed disc of Pt powder, which proved to be as stable as bulk Pt metal itself when used under the electrochemical conditions associated with the OER, or HER,, much unlike GC/carbon based electrodes.[14] Thus, in this paper we use this new pressed disc method to probe the electrochemical characteristics of a number of different metal oxides made from PGM and Earth Abundant Metal (EAM) salts using the Adams method. These pressed disc electrodes are probed not only as electrodes for the OER but also for the HER.

Results and Discussion

Material Characterisation

As already mentioned, the Adams method has been used previously for making oxides of PGMs, such as IrO_2, however, to our knowledge, this synthetic method for making crystalline metal oxides has not been applied to EAMs.[9-10, 15] Hence, the determination of the metal oxide structures synthesised using the Adams method in this study was an important first step in the characterisation of these materials. The powder X-Ray diffractograms for the Adams powders made in this study from the relevant metal precursors are illustrated in Figure 1.

The XRD patterns in Figure 1(a-d) reveals the Ru, Co, Ni and Mn Adams powders can be assigned to RuO_2, Co_3O_4, NiO and Mn_2O_3, respectively, the patterns for which have been reported previously[10a, 16]. The peaks for the RuO_2, Figure 1(a), are broad indicating that the RuO_2 structure is not highly crystalline, i.e. it has some amorphous character. XPS analysis of the oxide powders further confirms the results of the XRD analysis; see Supporting Information Section S1, Figure S1-2. BET surface areas of 132, 1.26, 22.4 and 11.3 m^2/g were determined for the respective samples.

Disc electrodes of all the Adams metal oxides were made by pressing the powders onto Pt powder. The role of the underlying pressed Pt disc is to provide a conducting medium between the electrode contact and the electroactive material. Although only a very small (<2%, see S1) of the pressed Pt disc is exposed to solution, it must not be highly electro-active itself. This feature is demonstrated by the LSV data illustrated in figure S8, section S5, which show that the bare pressed powdered Pt disc exhibited high OER and HER overpotentials – much higher than those electroactive materials under test - and therefore is a suitable current collector for this study.'

SEM-EDX analyses were conducted to determine the coverage of a metal oxide on the surface of a pressed Pt discs, which was typically > 98%. Figure 2 illustrates a typical set of SEM images of the surface of a pressed Pt disc with pressed electrocatalyst powder/PTFE missed top layer, in this case RuO_2; SEM images of the original powders are given in S2. After disc fabrication, for all the metal oxides, the morphology of the initial powder, see SEMs in Figure S3, was replaced by a continuous film of the oxide, ca. 30 μm thick, as illustrated in Figure 2 for RuO_2.

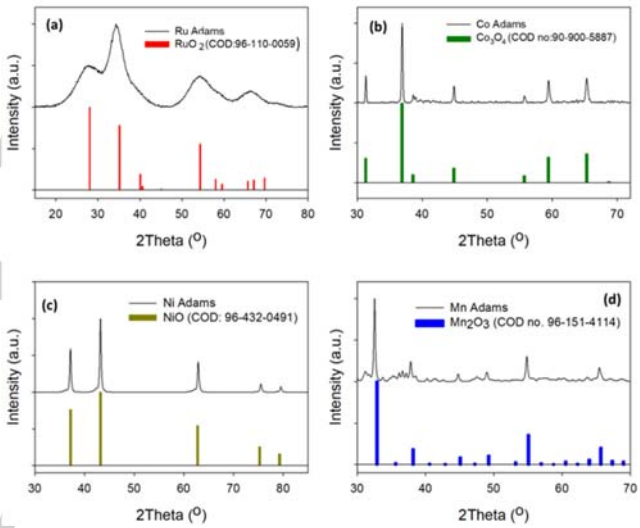

Figure 1. pXRD patterns of **(a)** Ru Adams **(b)** Co Adams **(c)** Ni Adams and **(d)** Mn Adams with crystallography open database (COD) references.

Figure 2(a) reveals that the pressed electrocatalyst surface is relatively smooth and. from the EDX map of the fluorine Kα1_2, see Figure 2(b), the larger particles on the surface of the disc are due to the PTFE binder, although, otherwise the PTFE appears evenly and finely dispersed throughout the pressed metal oxide surface. From an inspection of the images illustrated in Figure 2(c), it can be seen that the RuO_2 catalyst dominates the surface and is also evenly distributed across the surface of the supporting pressed Pt disc.

Figure 2. (a) SEM image of a typical AdamsRuO_2 powder on a Pt pressed disc in BS mode **(b)** EDX map of the F kα1_2 line showing the position of the PTFE

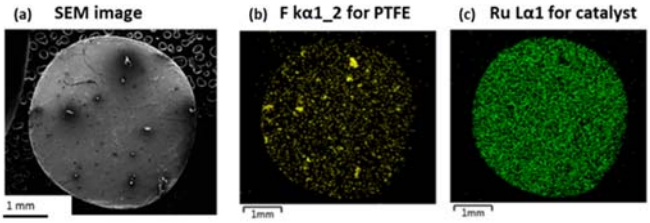

on the pressed Pt disc and **(c)** Ru Lα1 EDX map showing the position of the RuO_2 catalyst on the pressed Pt disc.

Electrochemical Performance

Prior to the OER and HER study the electrochemical surface areas (ECSAs) of the electrode discs were evaluated and found to be: 925, 70, 43 and 95 cm^{-2}, for the RuO_2, Co_3O_4, NiO and Mn_2O_3/pressed Pt discs, respectively, see also Table 1. The linear sweep voltammograms, LSVs, of each of the electrodes were conducted in 1 M NaOH for both the OER and HER and the results of this work are illustrated in Figures 3(a) and 4(a), respectively. The activity and stability of the Adams/pressed Pt disc towards OER and HER were characterised by their overpotentials at -/+10 mA cm^{-2}, respectively. The Tafel slopes, *b*, and electrocatalyst stabilities, over a period of 20 hours (chronopotentiometry), of all the electrodes were also determined and the results of this work are illustrated in Figures 3 and 4, respectively, and summarised in Table 1.

Oxygen Evolution Reaction

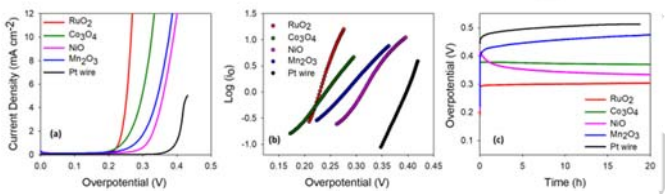

Figure 3. OER Properties of the Adams Powders on the pressed Pt discs and a Pt wire in 1M NaOH at 1500 rpm (a) Linear Sweep Voltammetry curves (b) Tafel plots (using the data in (a) and (c) chronopotentiometry curves (i = 10 mA cm^{-2}) .

'From the OER LSV curves, in Figure 3(a), and the Turnover Frequencies (TOF) values, see Figure S7 and Table S2, for the various metal oxides on the pressed discs, it appears that the RuO_2 and the Co_3O_4 electrocatalytic powders are the most active, with overpotential values, at 10 mA cm^{-2}, of 0.267 and 0.330 V and TOF values (at 0.30 V) of 0.4798 and 0.4162 s^{-1}, respectively. The high activity of the RuO_2 electrode is not too surprising given its very high electrochemical surface area (925 cm^{-2}). However, the latter feature makes the high activity of the Co_3O_4 all the more impressive, given its much lower ECSA value (70 cm^{-2}). All of the metal oxides tested appeared superior as electrocatalysts for the OER, compared to the pressed Pt disc electrode (i.e. with no electroactive species as a top cover), see η_{10} values in table 1 and Figure S8(a). The latter observation is not too surprising given that Pt, or more appropriately PtO_2 since the metal surface will be oxidised under these electrochemical conditions, is not known for its high electrocatalytic activity with regard to the OER.[17] XPS analysis of the pressed Pt disc, see S6, revealed the presence of 2.5 at% of PtO_x.

Tafel plots of the LSV data for all the metal oxides, illustrated in Figure 3(b), reveal a wide range of Tafel slopes, i.e. 30-86 mV dec^{-1}, and from these results, it appears that the RuO_2 exhibits the lowest Tafel slope, i.e. of 30 mV dec^{-1}, and that higher Tafel slope values are found for the other materials, see Table 1. Obviously, a key feature of any electrocatalyst is stability under prolonged use and so, in this work, chronopotentiometric curves were recorded for each of the electrodes when operated at a current density of 10 mA cm^{-2}, and these are illustrated in Figure 3(c). Encouragingly, from these plots, the RuO_2 and the Co_3O_4 electrodes show no change in OER overpotential over the 20 hour period, implying significant stability. Interestingly, the trend in activity of the Mn_2O_3 and the NiO is reversed during polarisation; in fact, the activities of these materials are reversed within the first hour of polarisation. The activity increase for NiO based materials has been noted before and is usually ascribed to iron impurities in the electrolyte;[1b, 18] while the slight decrease in the overpotential for the Mn_2O_3 electrode may be due to corrosion *via* the formation of higher unstable Mn oxidation states produced by the high OER potentials. Note that none of these Pt supported electrodes undergo a marked loss of activity during their prolonged stability trials, whereas, in contrast, such a marked change is often observed when using the same metal oxides powders drop cast onto GC.[19]

Hydrogen Evolution Reaction

The electrochemical activities of the different electrocatalysts reported here were also evaluated with regard to the HER in 1 M NaOH, and the results of this work are illustrated in Figure 4. Interestingly, as found in the OER study, the 'blank' pressed Pt powder disc, see Figure S8(b), is a poor electrocatalyst for the HER (η_{-10} = 225 mV) and vastly inferior to the Pt wire (η_{-10} = 70 mV). One possible reason for this is that the Pt pressed powder electrode comprises Pt particles with a thin coating of PtO_2, which still allows them to act a conducting support substrate, but interferes with their ability to mediate the HER. In all cases, the deposition of the Adams metal oxide powders onto the pressed Pt disc reveals them to be much more active as electrocatalysts with regard to the HER than the blank pressed Pt disc. the activity of the Mn_2O_3/pressed Pt disc outperforms that of the Pt wire for the HER, with η_{-10} = 61 mV for Mn_2O_3 compared to 70 mV for the Pt wire, respectively. The Co_3O_4 and RuO_2 on the pressed Pt discs electrodes also exhibit excellent HER characteristics, i.e. 0.10 and 0.095 V at -10 mA cm^{-2}, respectively, especially when compared to other Co_3O_4 and RuO_2 water reduction catalysts in the literature, see Table 1.[19] The poorest of the metal oxides tested, i.e. NiO, was not that different from the other metal oxides

reported in this study, i.e. η_{-10} = 140 mV, compared to 60-100 mV, see table 1.

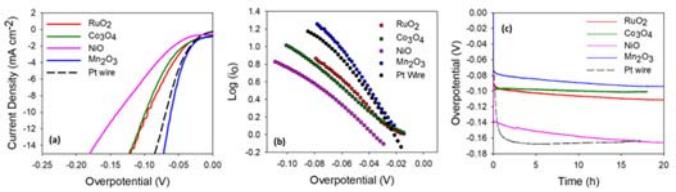

Figure 4. HER Properties of the Adams Powders on the pressed Pt discs and a Pt wire in 1M NaOH at 1500 rpm (a) Linear Sweep Voltammetry curves (b) Tafel plots (using the data in (a)) and (c) chronopotentiometry curves. All electrodes are pressed powders on Pt powder disc unless stated otherwise.

Tafel plots of the LSV data for the HER are illustrated in figure 4(b) and the values are listed in Table 1. These results, coupled with the TOF values in Table S2, show that Mn_2O_3 exhibits the lowest Tafel slope of 40 mV dec^{-1} and highest TOF (1.4 s^{-1}, at 0.06V), of the metal oxides tested, and hence, given it also had the lowest overpotential (i.e. η_{-10} = 61 mV) proceeds to evolve H_2 at a faster rate than the other Adams metal oxides and Pt wire. The higher Tafel slopes for RuO_2, Co_3O_4 and the NiO, see Figure 4(b) and Table 1, compared to the Mn_2O_3, indicates that the evolution of H_2 may proceed *via* a mixture of mechanistic steps which slows down the initial rate of H_2 evolution. The NiO electrode appears to lose activity with prolonged use, possibly due to its electroreduction. The chronopotentiometry curves over a prolonged time of approx. 18-20 hours for the Adams materials on the Pt discs, are illustrated in Figure 4(c), and reveal that all the metal oxides tested exhibit a high stability when used to mediate the HER. The very high overpotential (η_{-10} = 0.170 V) observed for the Pt wire in the chronopotentimetric studies was due to H_2 bubble formation, since the electrode was not spun, unlike the metal oxide disc electrodes. The TOF results for the different metal oxides, given in S4, show that the Mn_2O_3 has the highest HER TOF value of 1.3 s^{-1} and the Co_3O_4 has a comparable OER TOF value to that of RuO_2.

Table 1. Summary of OER and HER properties of the Adam metal oxide/pressed Pt electrodes in a three cell configuration in 1M NaOH.

Material on Pt pressed disc	OER [a] η_{10} (V)	HER [a] η_{-10} (V)	ECSA (cm^{-2})	BET surface area (m^2/g)	OER Tafel Slope (mV dec^{-1})	HER Tafel Slope (mV dec^{-1})
Ru Adams	0.267 **(0.380)**	0.09 **(0.125)**	925	132	30 **(64)**	60 **(n/a)**
Co Adams	0.330 **(0.500)**	0.100 **(0.350)**	70	1.26	72 **(61)**	80 **(n/a)**
Ni Adams	0.377 **(0.430)**	0.140 **(n/a)**	43	22.4	60 **(62)**	78 **(n/a)**
Mn Adams	0.367 **(0.530)**	0.061 **(n/a)**	95	11.3	80 **(70)**	40 **(n/a)**
Pt bare disc	0.450	0.225	9	n/a	86	150
Pt wire	0.47-0.50[b]	0.070	1.50	1.3	40	40

[a] Value in brackets are reported by others for the same metal oxides on a GC disc. RuO_2 and Co_3O_4 for HER[19]. All OER materials[20]. [b] taken from Figure 3(c).

From the OER and HER measurements, summarised in Table 1, it appears that the electrochemical activities, as measured by the overpotentials at ±10 mA cm^{-2}, of all the Adams metal oxides on the pressed Pt discs, are superior to the same metal oxides synthesied by different methods and deposited on glassy carbon substrates in current literature; examples of the previously reported characteristics of the latter are given in parentheses in Table 1.[19-20]

Solar-Driven Water Splitting

Finally, the optimum earth abundant materials from the OER and HER studies, summarised in Table 1, were investigated as overall water splitting catalysts in a 2 electrode cell. From Table 1, the best electrodes for the OER and the HER are the Co_3O_4/pressed Pt disc and the Mn_2O_3/pressed Pt disc, respectively. Hence the Co_3O_4 and the Mn_2O_3 on the pressed Pt discs were used as electrodes and immersed in 1 M NaOH in an air tight cell and connected to a solar cell illuminated by a 1.5 AM G solar simulator.

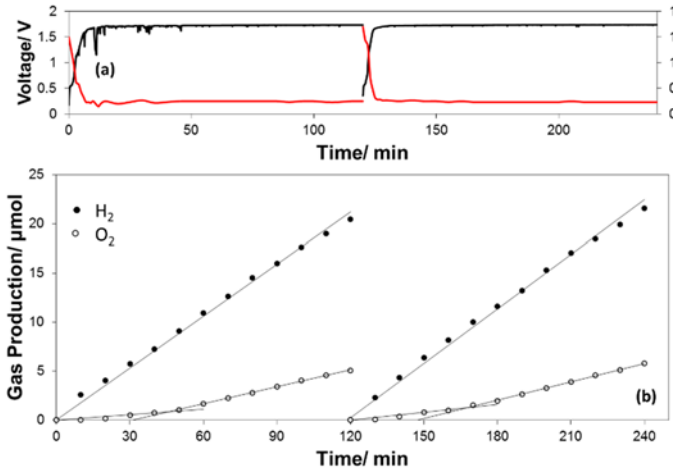

Figure 5 (a) Photovoltage and Photocurrent generated from the solar cell illumined by the 1.5 AM G solar simulator connected to the Co_3O_4/pressed Pt anode and the Mn_2O_3/pt pressed cathode and **(b)** Hydrogen and evolution gas generated from the solar cell connected to the Co_3O_4 and Mn_2O_3/pressed Pt discs in a gas tight cell under 1.5 AM (100 mW cm^{-2}) illumination determined by gas chromatography.

The photocurrent and the photovoltage generated by the solar driven water electrolysis cell with the Co_3O_4/pressed Pt anode and the Mn_2O_3/pressed Pt cathode were 0.65 mA and 1.73 V, respectively, and very stable, as illustrated by the potentiometric curves illustrated in Figure 5(a). The electrochemical efficiency of the H_2 was determined to be 100% by comparing the theoretical and actual moles generated by the solar driven cell using gas chromatography for the photo-cathodic reaction on the Mn_2O_3 based electrode, see Figure 5(b). The O_2 electrochemical efficiency was calculated to be ca. 67%, once the cell had been running for about 30 min, whereas before this it was typically only 30%. The reason for this initial low yield of O_2 is not clear, although adventitious oxidisable impurities could be one cause. For example, the purity of the NaOH used was 96% and so – with a 1 M solution – the level of impurities could be relatively high, i.e. >10 mM. Although the nature of these impurities are as yet unknown, others[18a] have identified iron salts as a potential contaminant of NaOH, which interfere in the OER reaction. The overall Solar to Hydrogen efficiency, STH, of this earth abundant material based silicon solar cell system for water splitting, was calculated to be 6.4 %, given[21] :

$$STH = i(mA\ cm^{-2}) \times 1.23 / P_{total}(mW\ cm^{-2}) \quad (1)$$

Where, i = photocurrent (5.2 mA cm^{-2}) and t_{total} = 100 mW cm^{-2}.

Conclusions

This work demonstrates that the earth abundant metal oxides, Co_3O_4, NiO and Mn_2O_3, can be fabricated by the Adams Fusion method, along with RuO_2. OER and HER electrodes of these oxides, fabricated using a previously reported[14] mechanical and solvent free method, using powder catalysts on pressed onto powdered Pt disc electrodes, were tested for activity with respect to the HER and OER. These electrochemical studies revealed that that the most active earth abundant metal oxides were Co_3O_4 and Mn_2O_3, for the OER and HER, respectively. In addition, for both the OER and HER, these metal oxides are very stable under prolonged polarisation at a current density of 10 mA cm^{-2}. The Co_3O_4 and Mn_2O_3 pressed Pt disc electrodes, when utilised as electrocatalysts in a solar-driven, silicon-solar cell water splitting cell, were able to split water with a 100% electrochemical efficiency for H_2 and with a 6% solar to hydrogen efficiency.

Experimental Section

Materials

The metal salts used to make the oxides using the Adams method were: manganese (II) chloride tetrahydrate (Sigma Aldrich, ReagentPlus ≥99%), iridium (III) chloride hydrate (Sigma Aldrich, Reagent grade), ruthenium (III) chloride hydrate (Sigma Aldrich, ReagentPlus ≥99%), nickel (II) nitrate hydrate (Sigma Aldrich, metals basis 99.999%) and cobalt (II) chloride (Sigma Aldrich, 97%); the $NaNO_3$ used to create the melt was also obtained from Sigma Aldrich (≥99%). The polymer used to make the pressed discs of the metal oxide electrocatalysts was poly(tetrafluoroethylene) (PTFE) powder (Sigma Aldrich, 1µm particle size), which also utilised platinum powder (Alfa Aesar, 200 mesh, metals basis, 99.98%). The electrolyte used in all this work was 1 M NaOH, which was made up using sodium hydroxide pellets (96%, Scientific and Chemical Supplies ltd) and doubly-distilled, deionized water. The Pt wire which was used as a benchmark electrode for the HER was obtained from Goodfellows, UK.

Adams Synthetic Method

The metal (Ru, Ir, Co, Ni and Mn) oxide powders were fabricated using a modified Adams method previously employed in our group[10a] Briefly, 1 g of the relevant metal salt and 20 g sodium nitrate were dissolved in approximately 15 ml of water in a crucible and sonicated for 30 minutes, using an ultrasound bath to ensure everything was completely dissolved. The reaction solution was then placed into a muffle furnace and heated for 25 minutes at 500°C, previously using an initial ramp rate of 20°C per minute for 25 minutes to reach the temperature of 500°C. The crucible was allowed cool overnight and then the metal oxide powdered product extracted and cleaned by dissolving up the melt in water and centrifuging the dispersion, decanting off the excess water, replacing it with clean water and repeating the process until the powder was free of nitrate. The powder was then dried at 100°C in an oven and stored until used.

Characterisation Parameters

Powder X Ray Diffraction (XRD) of the Adams powders was carried out using a Bruker Advanced D8 ECO with a Copper (Cu) Kα source (λ = 1.5418 Å) at 40 kV and 40 mA. Brunauer–Emmett–Teller isotherms of the Adams powders were obtained using a Micromeritics Tristar 3020 BET instrument using N_2 as the absorption gas. Scanning Electron Microscopy (SEM) measurements were carried out using a FEI Quanta™ 250 SEM with a spot size of 4 mm, working distance of 10 mm and an accelerating voltage of 20 kV. Energy dispersive X-Ray (EDX) mapping was carried out using an EDX detector from Oxford Instruments coupled to the SEM instrumentation. The X-Ray Photoelectron Spectroscopy (XPS) was

carried out using a VG Scientific ESCA Lab MKII system, with an Al Kα X -ray source (1486.7 eV). For survey scans, an analyser pass energy of 200 eV was used, while a pass energy of 20 eV was used to obtain high resolution spectra of characteristic core levels. All spectra were calibrated to the C1s peak.

Pressed Rotating Disc Electrode Fabrication

In this work, a pressed disc electrode (4 mm diameter) was prepared by first inserting 300 mg of Pt powder into an IR pellet press die (Specac). And gently pressing it down by hand using the stainless steel IR die rod. Then, an intimate mixture of 0.9 mg of the Adams metal oxide powder under test and 0.1 mg of PTFE powder, an electrochemically inert organic binder, were placed on top of the pressed Pt powder in the die. The contents of the die were then subjected to a pressure of 2 tonnes for 10 s, using a hydraulic IR press, so as to yield at pressed disc of the powdered catalyst with an underlying Pt (pressed powder) conducting support.

Electrochemical Parameters

All electrochemical measurements were conducted in a three electrode cell consisting of a Rotating Disc Electrode (RDE) as the working electrode, a graphite rod as the counter electrode and an Hg/HgO reference electrode. As noted earlier, the electrolyte was 1M NaOH solution and was de-gassed with Ar gas for 15 mins prior to each measurement. The RDE assembly (ALS co. Ltd) employed in this work allowed replaceable discs of the working electrode to be used. For the Linear Sweep Voltammetry (LSV) measurements, the fabricated metal oxide disc inserted into the RDE set up was rotated at 1500 rpm and a scan rate of 0.1 mV/sec was applied. All LSV curves were compensated for iR drop. The resistance values were determined by Electrochemical Impedance Spectroscopy (EIS) in a non-Faradaic region of the cyclic voltammogram (CV) of the electrocatalyst. The EIS measurements were conducted in the frequency range of 10000 Hz to 0.1 Hz. Typical resistance values for all metal oxide electrodes were between 7-11 Ω. With regard to EIS measurements, see S7 for an example set of data and calculation for the RuO_2 electrode. for Electrochemical surface areas (ECSA) experiments were carried out by performing multiple CV experiments in a non-Faradaic region (typically in the 0–0.3V vs. Hg/HgO region) at various scan rates (typically 1–200 mV/s). The ECSA of each electrode was determined from a study of its cyclic voltammogram as a function of scan rate in its non-Faradaic region where just charging, and no redox reactions, occur. However, the same active sites responsible for the buildup of charge in the non-Faradaic region may not be the same active sites responsible for the redox reaction under investigation. As a consequence, it should be noted that whilst a useful guide, calculated current densities based on ECSA may over, or under, compensate the activity of the electrocatalyst. With regard to ECSA measurements, see S3 for an example set of data and calculation for the RuO_2 electrode.. Likewise, Brunauer Emmett teller (BET) Surface Area (SA) values give a good indication of surface area of a powder but do not necessarily directly correlate with the active sites of a pressed disc of the powdered material; indeed, in practice current densities based on BET SAs regularly overestimate the activity of the electrode catalytic materials[20]Thus, in this study, we report current densities based on geometric area only, as is common practice; although some reference to BET SA and ECSA is made in the discussion of results.

The prolonged stability (chronopotentiometric) tests were run by applying a constant current density of ±10 mA cm^{-2} in 1 M NaOH (for the OER and HER, respectively) and monitoring the applied voltage as a function of time. The current densities reported in this current study have been normalized by geometric area and all working electrodes have a diameter of 4 mm.

The solar-driven water splitting H_2 and O_2 evolution rates of the optimum earth abundant electrodes were evaluated using a GC-2014 Shimadzu gas chromatography with an Alltech CTR I Column (2.0 m, 5.0 mm ID) at a temperature of 33°C and a Thermal conductivity Detector (TCD) at a temperature of 140°C. Ar was used as the carrier gas at a flow rate of 65 mL/min. The injection port was at a constant temperature of 120 °C and the injection volume for each sample was 100 µL. The solar cell used in the solar-driven water splitting experiments was purchased from RS components. The 1.5 AM solar simulator model SS150W was from Sciencetech.

Acknowledgements

The authors would like to thank Mr. Conor Cullen and Prof Georg Duesberg from Trinity College Dublin for carrying out the XPS analysis.

Keywords: Electrochemistry; Sustainable chemistry; catalysis, water-splitting.

[1] a) I. Dincer, C. Acar, *Int. J. Hydrogen Energy* **2015**, *40*, 11094-11111; b) M. Gong, H. Dai, *Nano Res.* **2015**, *8*, 23-39; cM. Shao, Q. Chang, J.-P. Dodelet, R. Chenitz, *Chem. Rev.* **2016**, *116*, 3594-3657.

[2] a) M. E. G. Lyons, R. L. Doyle, M. P. Browne, I. J. Godwin, A. A. S. Rovetta, *Current Opinion in Electrochemistry* **2017**, *1*, 40-45; b) K. Zeng, D. Zhang, *Prog. Energy Combust. Sci.* **2010**, *36*, 307-326; c) C. C. L. McCrory, S. Jung, I. M. Ferrer, S. M. Chatman, J. C. Peters, T. F. Jaramillo, *J. Am. Chem. Soc.* **2015**, *137*, 4347-4357; d) C. C. L. McCrory, S. Jung, J. C. Peters, T. F. Jaramillo, *J. Am. Chem. Soc.* **2013**, *135*, 16977-16987; e) J. Luo, J.-H. Im, M. T. Mayer, M. Schreier, M. K. Nazeeruddin, N.-G. Park, S. D. Tilley, H. J. Fan, M. Grätzel, *Science* **2014**, *345*, 1593-1596.

[3] a) H. Nolan, N. McEvoy, M. O'Brien, N. C. Berner, C. Yim, T. Hallam, A. R. McDonald, G. S. Duesberg, *Nanoscale* **2014**, *6*, 8185-8191; b) J. D. Benck, T. R. Hellstern, J. Kibsgaard, P. Chakthranont, T. F. Jaramillo, *ACS Catalysis* **2014**, *4*, 3957-3971.

[4] a) M. P. Browne, J. M. Vasconcelos, J. Coelho, M. O'Brien, A. A. Rovetta, E. K. McCarthy, H. Nolan, G. S. Duesberg, V. Nicolosi, P. E. Colavita, M. E. G. Lyons, *Sustainable Energy & Fuels* **2017**, *1*, 207-216; b) L. C. Seitz, D. Nordlund, A. Gallo, T. F. Jaramillo, *Electrochim. Acta* **2016**, *193*, 240-245; c) G.-Q. Han, Y.-R. Liu, W.-H. Hu, B. Dong, X. Li, X. Shang, Y.-M. Chai, Y.-Q. Liu, C.-G. Liu, *J. Electrochem. Soc.* **2016**, *163*, H67-H73; d) S. Lian, M. P. Browne, C. Dominguez, S. N. Stamatin, H. Nolan, G. S. Duesberg, M. E. G. Lyons, E. Fonda, P. E. Colavita, *Sustainable Energy & Fuels* **2017**, *1*, 780-788; e) X. Shang, K.-L. Yan, S.-S. Lu, B. Dong, W.-K. Gao, J.-Q. Chi, Z.-Z. Liu, Y.-M. Chai, C.-G. Liu, *J. Power Sources* **2017**, *363*, 44-53; f) K.-L. Yan, J.-Q. Chi, Z.-Z. Liu, B. Dong, S.-S. Lu, X. Shang, W.-K. Gao, Y.-M. Chai, C.-G. Liu, *Inorganic Chemistry Frontiers* **2017**, *4*, 1783-1790.

[5] X. Gao, H. Zhang, Q. Li, X. Yu, Z. Hong, X. Zhang, C. Liang, Z. Lin, *Angewandte Chemie - International Edition* **2016**, *55*, 6290-6294.

[6] M. G. Walter, E. L. Warren, J. R. McKone, S. W. Boettcher, Q. Mi, E. A. Santori, N. S. Lewis, *Chem. Rev.* **2010**, *110*, 6446-6473.

[7] a) M.-Q. Wang, C. Ye, S.-J. Bao, Z.-Y. Chen, H. Liu, M.-W. Xu, *ChemCatChem*, (http://dx.doi.org/10.1002/cctc.201700935); b) L. Liu, Z. Jiang, L. Fang, H. Xu, H. Zhang, X. Gu, Y. Wang, *ACS Applied Materials & Interfaces* **2017**, *9*, 27736-27744.

[8] M.-R. Gao, X. Cao, Q. Gao, Y.-F. Xu, Y.-R. Zheng, J. Jiang, S.-H. Yu, *ACS Nano* **2014**, *8*, 3970-3978.

[9] E. Oakton, D. Lebedev, A. Fedorov, F. Krumeich, J. Tillier, O. Sereda, T. J. Schmidt, C. Coperet, *New J. Chem.* **2016**, *40*, 1834-1838.

[10] a) A. Mills, D. Hazafy, S. Elouali, C. O'Rourke, *Journal of Materials Chemistry A* **2016**, *4*, 2863-2872; b) E. Oakton, D. Lebedev, M. Povia, D. F. Abbott, E. Fabbri, A. Fedorov, M. Nachtegaal, C. Copéret, T. J. Schmidt, *ACS Catalysis* **2017**, *7*, 2346-2352.

[11] S. Geiger, O. Kasian, A. M. Mingers, S. S. Nicley, K. Haenen, K. J. J. Mayrhofer, S. Cherevko, *ChemSusChem*, n/a-n/a.

[12] M. A. Sayeed, A. P. O'Mullane, *RSC Advances* **2017**, *7*, 43083-43089.

[13] M. P. Browne, C. Domínguez, P. E. Colavita, *Current Opinion in Electrochemistry* **2017,**https://doi.org/10.1016/j.coelec.2017.09.012.

[14] M. P. Browne, C. O'Rourke, A. Mills, *Electrochem. Commun.* **2017**, *85*, 1-5.

[15] V. Voorhees, R. Adams, *J. Am. Chem. Soc.* **1922**, *44*, 1397-1405.

[16] a) Y. Y. Liang, *Nat. Mater.* **2011**, *10*, 780-786; b) M. A. Peck, M. A. Langell, *Chem. Mater.* **2012**, *24*, 4483-4490; c) M. P. Browne, H. Nolan, B. Twamley, G. S. Duesberg, P. E. Colavita, M. E. G. Lyons, *ChemElectroChem* **2016**, *3*, 1847-1855.

[21] Z. Chen, H.N. Dinh, E, Miller in Photochemical Water Splitting Standards, Experimental Methods and Protocols, Vol.1, Springer, 2013, pp 8-9.

[17] a) T. Reier, M. Oezaslan, P. Strasser, *ACS Catalysis* **2012**, *2*, 1765-1772; b) M. Favaro, C. Valero-Vidal, J. Eichhorn, F. M. Toma, P. N. Ross, J. Yano, Z. Liu, E. J. Crumlin, *Journal of Materials Chemistry A* **2017**, *5*, 11634-11643.

[18] a) M. P. Browne, S. Stafford, M. O'Brien, H. Nolan, N. C. Berner, G. S. Duesberg, P. E. Colavita, M. E. G. Lyons, *Journal of Materials Chemistry A* **2016**, *4*, 11397-11407; b) D. A. Corrigan, *J. Electrochem. Soc.* **1987**, *134*, 377-384; c) S. Klaus, Y. Cai, M. W. Louie, L. Trotochaud, A. T. Bell, *Journal of Physical Chemistry C* **2015**, *119*, 7243-7254.

[19] H. Liu, G. Xia, R. Zhang, P. Jiang, J. Chen, Q. Chen, *RSC Advances* **2017**, *7*, 3686-3694.

[20] S. Jung, C. C. L. McCrory, I. M. Ferrer, J. C. Peters, T. F. Jaramillo, *Journal of Materials Chemistry A* **2016**, *4*, 3068-3076.

Entry for the Table of Contents

ARTICLE

Sunlight Generated Energy: Solar driven water splitting in alkaline media using high surface area Co_3O_4 and Mn_2O_3 Earth abundant metal oxides with a 100% electrochemical efficiency for H_2 and 6% overall solar to hydrogen efficiency for the two electrode device.

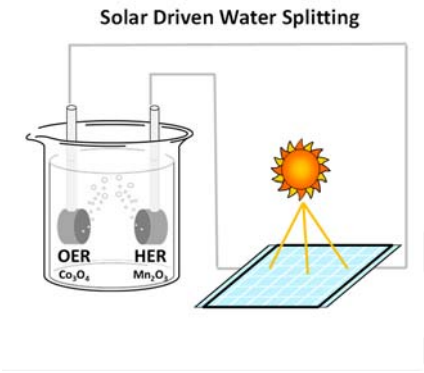

*M. P. Browne, C. O'Rourke and A. Mills**

Page No. – Page No.

Adams Metal Oxide Catalysts for Solar Driven Water Splitting

Supporting Information

Adams Metal Oxide Catalysts for Solar Driven Water Splitting

M. P. Browne, [a] C. O'Rourke [a] and A. Mills*[a]

S1. Further structural characterisation

The XPS survey of the Adams metal oxides/pressed Pt discs can be observed in Figure S1. All of the survey scans for the various discs display peaks at characteristic energies O1s and C1s. Additionally; the surveys for the RuO_2, Co_3O4, NiO and Mn_2O_3 pressed Pt discs only show the corresponding core level which are Ru3p, Co2p, Ni2p and Mn2p, respectively. This result suggests that no cross contamination of the oxides occurred during the fabrication of the films.

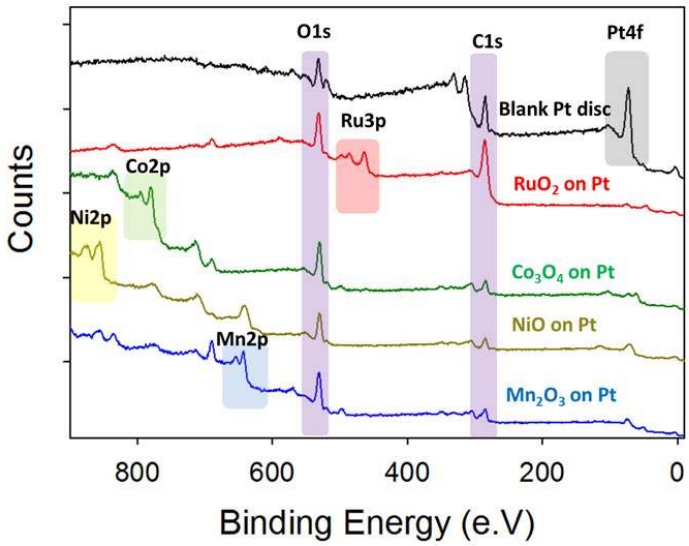

Figure S1. XPS Survey of all Adams powders on the pressed Pt discs

The representative core level scans of the main metal oxide in each of the Adams metal oxide /pressed Pt disc can be observed in Figure S2(a-d). The Ru $3p_{3/2}$ peak of the Ru Adams/pressed Pt disc was fitted with contributions correlating to Ru^{4+} (RuO_2) according to Morgan *et al*,[1] Figure S2(a). Additionally, the experimental $Co2p_{3/2}$ peak associated with the Co Adams/pressed Pt disc was fitted with $Co^{+2/+3}$ (Co_3O_4) contributions, Figure S2(b), while the Mn $2p_{3/2}$ core-level of the Mn Adams/pressed Pt disc was fitted to a Mn^{3+} (Mn_2O_3) multiplet set, as shown in Figure S2(c). The $Ni2p_{3/2}$ peak was fitted with contributions associated with Ni^{2+} (NiO), Figure S2(c). The Co_3O_4, Mn_2O_3 and the NiO fittings were done in according to

Grosvenor *et al*.[2] All of the XPS fittings of the Adams/pressed Pt disc verify the results of the XRD analysis, Figure 1 in the main manuscript.

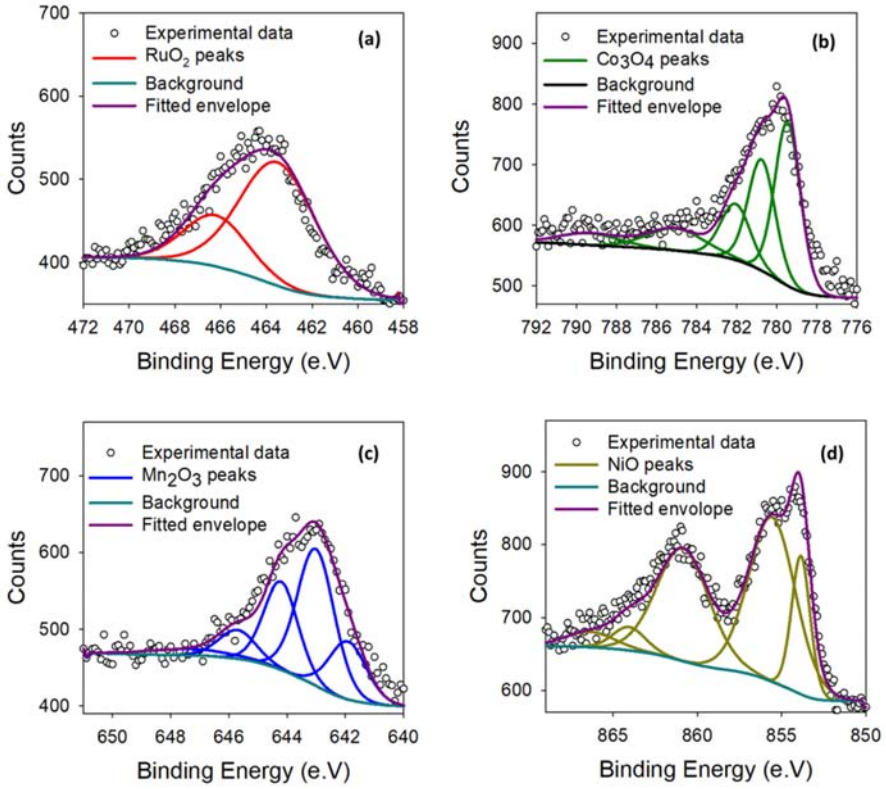

Figure S2. X-Ray Photoelectron Spectroscopy of the Adams powders on the pressed Pt disc**(a)** RuO_2 **(b)** Co_3O_4 **(c)** Mn_2O_3 and **(d)** NiO

Table S1. Maximum Pt% on the surface of the Pt discs

Adams/Pt pressed disc	**XPS core level**	**Pt % on surface of disc**
Ru	**Ru3p**	1.24
Co	**Co2p**	1.35
Ni	**Ni2p**	2.07
Mn	**Mn2p**	1.72

XPS was also undertaken to calculate the minimum amount of Pt on the surface of the disc after the metal oxide was pressed onto the Pt disc, Table S1. XPS is a surface sensitive technique and only probes the top 2-10 nm of a film. Hence, if Pt metal could be detected through XPS the probability of the Pt in contact with the electrolyte during the OER/HER measurements would be high and may affect the measurement. The Pt4f core level peak resides between 70 –78 eV and exists in a multiplet set due to the spin orbit coupling in the f orbital. The area associated with the Pt4f core level region for each of the Adams/pressed discs was determined and related to the O1s peak and the relevant metal oxide core level associated with that Adams/pressed Pt disc to calculate the maximum Pt% on the surface of the Adams samples. Additionally, From Table 1, it is evident that the maximum Pt% is between 1-2%. Subsequently, this result also shows the reproducibility of the Adams/pressed Pt discs from disc to disc fabrication as the Pt% variation is negligible; the standard deviation of the Pt% on the Adams/pressed Pt discs in Table 1 is 0.35%.

One must note that the area associated with the C1s peak was not taken into account when calculating the Pt% as the C1s peak overlapped with the Ru3d peaks for the Ru Adams/pressed Pt disc therefore the contribution from all of the C1s peaks were excluded from the Pt% determination.

S2. Further Microscopy studies

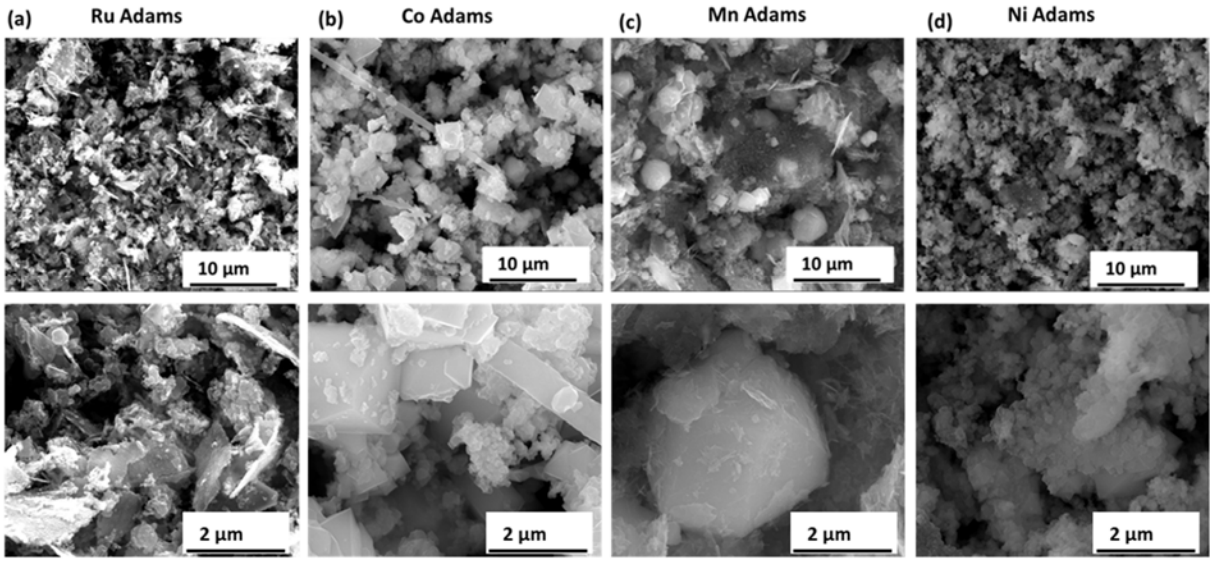

Figure S3. SEM images of the Adams powders **(a)** RuO_2 **(b)** Co_3O_4 **(c)** Mn_2O_3 and **(d)** NiO

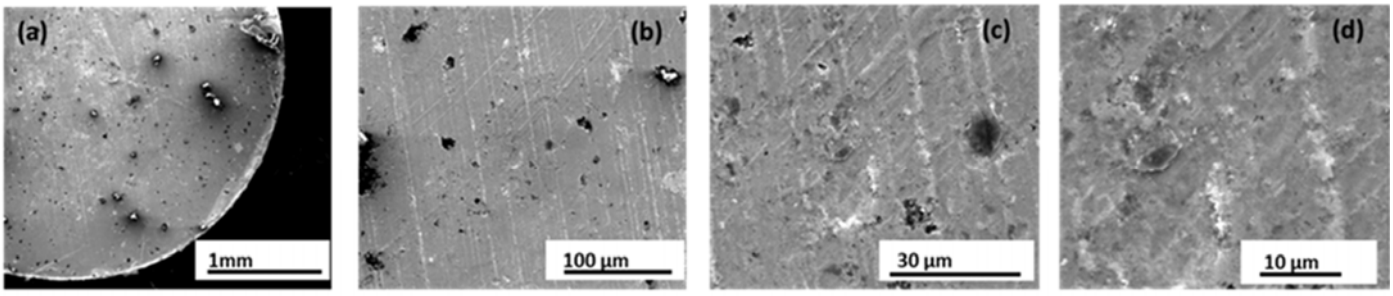

Figure S4. SEM Images of the Adams RuO_2/Pt pressed disc at various magnifications **(a)** 1mm **(b)** 100 µm **(c)** 30 µm and **(d)** 10 µm

Adams powder	Average Particle Sizes
RuO_2	Particles - 89 ± 10 nm Flakes - 1.8 – 2.0 µm
Co_3O_4	Octahedra* - 2.2 µm Debris - 134 – 238 nm
Mn_2O_3	Particles - 3.2 – 3.8 µm Flakes - 271 – 582 nm
NiO	Particles - 134 ± 30 nm

*: H. Xu, J. X. Wu, Y. Chen, W. J. Jing, B. Q. Zhang, 'Synthesis and catalytic performance of Co_3O_4 particles with octahedral crystal shape', *Ionics*, 21 (2015) 1495-1500

S3. Calculating the Electrochemical Surface Area (ECSA)

The Electrochemical Surface Area (ECSA), in this study, was determined using cyclic voltammetry/capacitance measurements, in a manner similar to previous published reports.[3] The ECSA is calculated from the equation below as follows[3a];

$$ECSA = \frac{C_{DL}}{C_S}$$

Where C_S is the specific capacitance and has a value of 0.04 mF cm^{-2}.[3a, 3b] Further information on the determination of the ECSA can be found papers reported by Jaramillo *et al*.[3a, 3b]

Briefly, experimentally, the ECSA was determined by recording CVs in a potential region where no Faradaic processes occur at various scan rates, Figure S3(a). The Double Layer Capacitance (C_{DL}) was determined by plotting the measured current at a specific potential over a range of scan rates, Figure S3(b). The slope obtained equaled the (C_{DL}). An example for calculating the double layer capacitance using the RuO_2 Adams powder on the pressed Pt disc, and hence the ECSA, can be observed below, Figure S3.

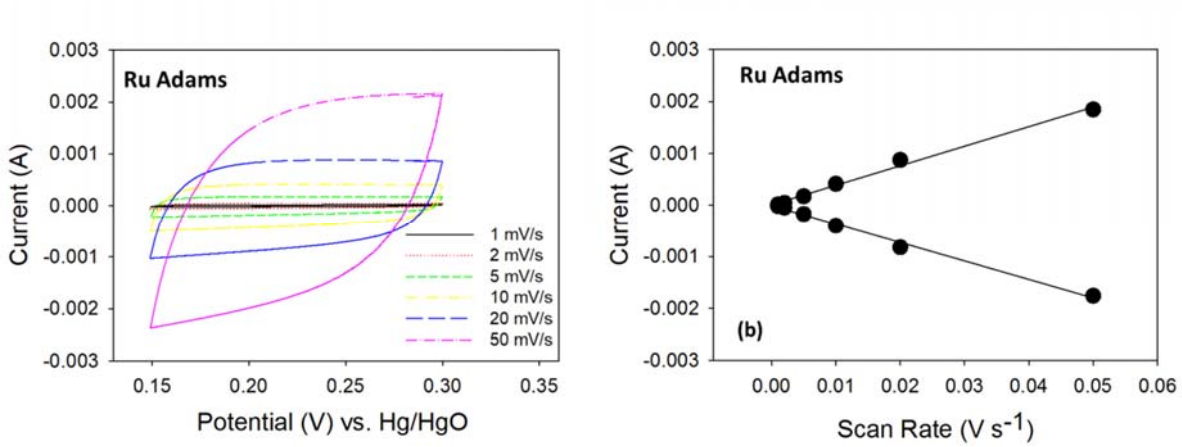

Figure S5. Double layer capacitance (C_{DL}) measurements for the RuO_2 Adams Powder on the pressed Pt discs **(a)** CVs taken at a range of scan rates and **(b)** Capacitance curves for this data were then plotted and the slope determined.

The summary of the ESCA values for the Adam metal oxide/Pt pressed discs can be found in the main manuscript in Table 1.

S4. Calculating the Turnover Frequency (TOF) value

The calculated turnover frequency for an electrochemical process, i.e. TOF, provides a measure of the material's ability to produce oxygen per active site per unit time. Thus, TOF are related to the current density (i.e. the rate of the electrochemical process) and the charge density, which provides a measure of the density of the electrochemically active sites on the electrode. Hence the TOF number is a rate per unit active material. Thus, in this work, the TOF was calculated at an overpotential of 0.30 V and -0.06 V for the OER and HER, respectively, using the following equations:

$$TOF\ OER = J_E/4Q$$

$$TOF\ HER = \ J_E/2Q$$

where J_E is the current density at the potential *E*, *Q* is the charge density associated with the non-faradic and redox processes occurring on the electrode and the multiplication factor 4 or 2 is used, as the OER and HER is a four or two electron transfer reaction.[4]

The Charge (Q) can be calculated from integrating the oxidation or reduction sweep of a cyclic voltammogram and a typical example can be observed in Figure S6 below. The area shaded in blue represents the oxidation region where the charge was calculated from in this study. The J_E can be determined from the LSV curves. All the metal oxides were analysed in this way, the results of which are illustrated in figure S6 and summarised in table S2.

Table S2. TOF values for all materials

Adams/Pt pressed disc	**OER TOF (s^{-1})**	**HER TOF (s^{-1})**
Ru	0.4798	0.1063
Co	0.4162	0.5448
Mn	0.1436	1.3988
Ni	0.0994	0.6250

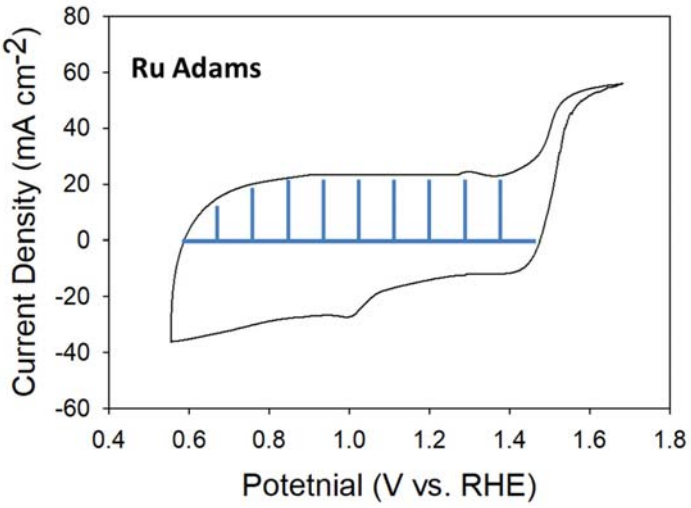

Figure S6. CV for the RuO_2 Adams Powder on the pressed Pt discs showing the region in blue where the charge (Q) is calculated.

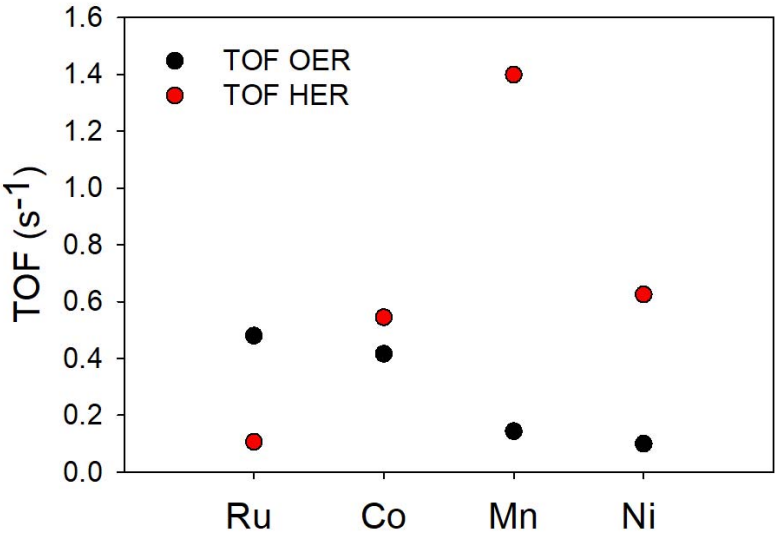

Figure S7. TOF values for all of the metal oxide on the pressed Pt disc for the OER and HER

S5. OER and HER performance of the bare pressed Pt disc

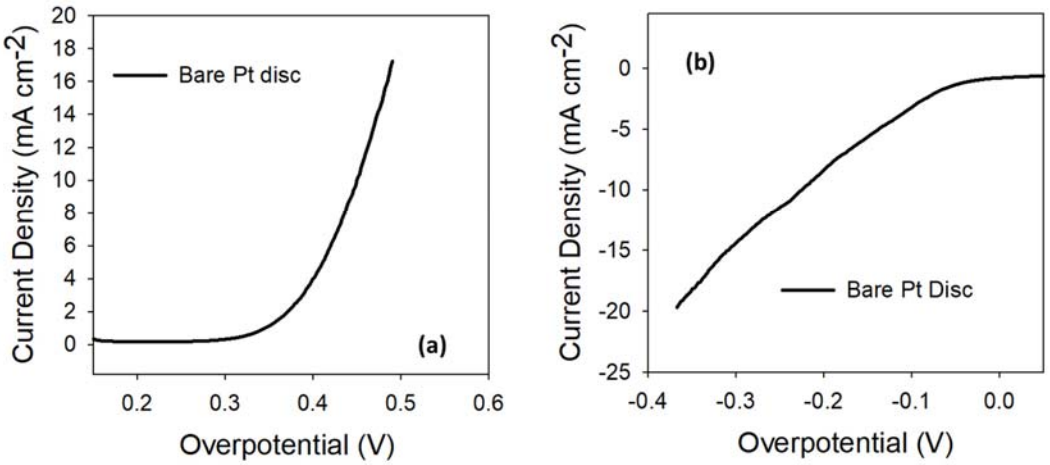

Figure S8. LSV of the bare Pt disc for **(a)** OER and **(b)** HER

The role of the bare pressed Pt disc is to act as a current collector for metal oxides. The bare Pt disc exhibit poor OER and HER overpotentials therefore can act as a suitable current collector in this study, Figure S9 and Table 1 in the main manuscript.

S6. Determining if there is PtO_x on the surface of the bare Pt disc

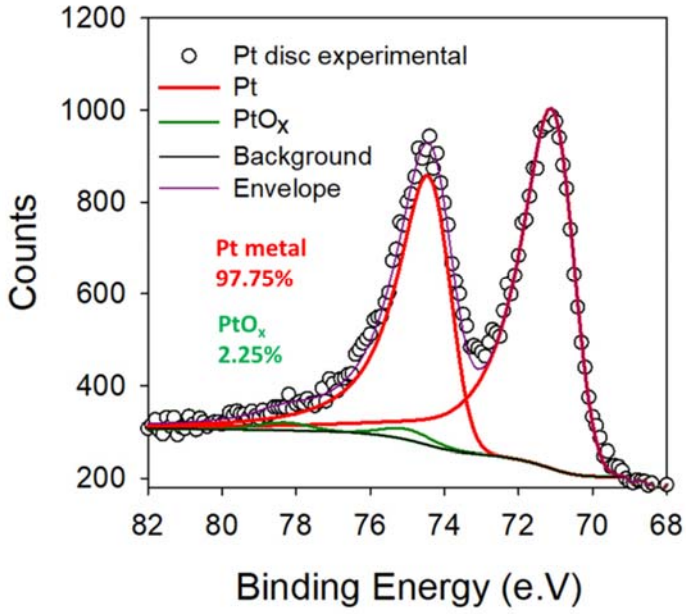

Figure S9. XPS core of Pt4f for the bare Pt pressed disc

S7. Calculating the Solution Resistance

The solution resistance (Rs) is determined by Electrochemical Resistance Spectroscopy (EIS). The Rs value is taken from the Nyquist plot where the plot intersects both the Y and X axis at high frequencies as outlined by Boettcher *et al.* in a recent review.[5] In Figure S2, a typical Nyquist plot can be observed for a RuO_2 Adams Powder on the pressed Pt discs used in this study.

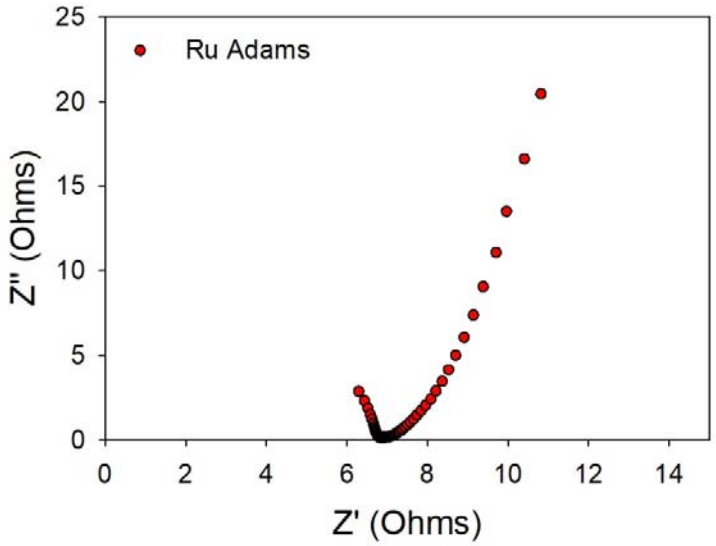

Figure S10. Nyquist plot for the RuO_2 Adams Powder on the pressed Pt discs

The summary of the Rs values for the Adam metal oxide/Pt pressed discs can be found in the main manuscript in Table 1.

References

[1] D. J. Morgan, *Surf. Interface Anal.* **2015**, *47*, 1072-1079.

[2] a) A. P. Grosvenor, M. C. Biesinger, R. S. C. Smart, N. S. McIntyre, *Surf. Sci.* **2006**, *600*, 1771-1779; b) M. C. Biesinger, B. P. Payne, A. P. Grosvenor, L. W. M. Lau, A. R. Gerson, R. S. C. Smart, *Appl. Surf. Sci.* **2011**, *257*, 2717-2730.

[3] a) C. C. L. McCrory, S. Jung, I. M. Ferrer, S. M. Chatman, J. C. Peters, T. F. Jaramillo, *J. Am. Chem. Soc.* **2015**, *137*, 4347-4357; b) C. C. L. McCrory, S. Jung, J. C. Peters, T. F. Jaramillo, *J. Am. Chem. Soc.* **2013**, *135*, 16977-16987; cM. W. Louie, A. T. Bell, *J. Am. Chem. Soc.* **2013**, *135*, 12329-12337.

[4] M. P. Browne, S. Stafford, M. O'Brien, H. Nolan, N. C. Berner, G. S. Duesberg, P. E. Colavita, M. E. G. Lyons, *Journal of Materials Chemistry A* **2016**, *4*, 11397-11407.

[5] M. B. Stevens, L. J. Enman, A. S. Batchellor, M. R. Cosby, A. E. Vise, C. D. M. Trang, S. W. Boettcher, *Chem. Mater.* **2017**, *29*, 120-140.